Pedro J. Lee, Martin F. Lambert, Angus R. Simpson, John P. Vitkovsky and James Liggett
Experimental verification of the frequency response method for pipeline leak detection

Experimental verification of the frequency response method of leak detection

by

Lee, P.J., Lambert, M.F., Simpson, A.R. and Vítkovský, J.P.

Journal of Hydraulic Research

Experimental verification of the frequency response method for pipeline leak detection

Vérification expérimentale de la méthode de réponse en fréquences pour la détection de fuite de canalisation

PEDRO J. LEE, Lecturer, Department of Civil Engineering, University of Canterbury, Private Bag 4800, Christchurch, New Zealand. E-mail: pedro.lee@canterbury.ac.nz (author for correspondence)

MARTIN F. LAMBERT, Associate Professor, Centre for Applied Modelling in Water Engineering, School of Civil & Environmental Engineering, The University of Adelaide, Adelaide, SA 5005, Australia. Tel.: **+** 61 8 8303 5838; fax: **+** 61 8 8303 4359; e-mail: mlambert@civeng.adelaide.edu.au

ANGUS R. SIMPSON, Associate Professor, Centre for Applied Modelling in Water Engineering, School of Civil & Environmental Engineering, The University of Adelaide, Adelaide, SA 5005, Australia. Tel.: **+** 61 8 8303 5874; fax: **+** 61 8 8303 4359; e-mail: asimpson@civeng.adelaide.edu.au

JOHN P. VÍTKOVSK†, Research Associate, Centre for Applied Modelling in Water Engineering, School of Civil & Environmental Engineering, The University of Adelaide, Adelaide, SA 5005, Australia. Tel.: **+** 61 8 8303 4324; fax: **+** 61 8 8303 4359; e-mail: jvitkovs@civeng.adelaide.edu.au

JAMES LIGGETT, Professor Emeritus, School of Civil & Environmental Engineering, Cornell University, Ithaca, NY 14853-3501, USA. E-mail: jal8@cornell.edu

ABSTRACT

This paper presents an experimental validation of the frequency response method for pipeline leak detection. The presence of a leak within the pipe imposes a periodic pattern on the resonant peaks of the frequency response diagram. This pattern can be used as an indicator of leaks without requiring the "no-leak" benchmark for comparison. In addition to the experimental verification of the technique, important issues, such as the procedure for frequency response extraction and methods for dealing with frequency-dependent friction are considered in this paper. In this study, transient signals are generated by a side-discharge solenoid valve. Non-linearity errors associated with large valve movements can be prevented by a change in the input parameter to the system. The optimum measuring and generating position for two different system boundary configurations—a symmetric and an antisymmetric system— are discussed in the paper and the analytical expression for the leak-induced pattern in these two cases is derived.

RÉSUMÉ

Cet article présente une validation expérimentale de la méthode de réponse en fréquences pour la détection de fuites de canalisation. La présence d'une fuite dans le tuyau induit une périodicité sur les crêtes résonnantes du diagramme de réponse en fréquences. Cette configuration peut être utilisée comme indicateur de fuite sans exiger un benchmark de "non-fuite" pour comparaison. En plus de la vérification expérimentale de la technique, des questions importantes, telles que le procédé d'extraction de la réponse en fréquence et les méthodes pour traiter le frottement lié aux fréquences sont considérés dans cet article. Dans cette étude, des signaux transitoires sont produits par une vanne latérale en solénoïde. Les erreurs de non-linéarité associées à des mouvements amples de la vanne peuvent être évités par un changement des paramètres d'entrée au système. La position optimale de mesure et de génération pour deux différentes configurations du système aux limites—un système symétrique et antisymmétrique—est discutée dans le papier et l'expression analytique du modèle induit de fuite dans ces deux cas est élaborée.

Keywords: Leakage, frequency response, linear systems, transients, water pipelines, resonance.

1 Introduction

All systems must rely on the speed and efficiency of a fault monitoring process for their continuous operation. The fast detection of problems within the system allows for efficient containment strategies, minimizing the resulting cost and damage. The problem of pipeline leakage is an example of where a good fault detection system is important for the long-term operation of the system. The use of fluid transients (water hammer waves) for this purpose is an attractive development in the field due to their high speed and operational range.

Publications proposing different strategies of fluid transient leak detection include inverse transient analysis (Liggett and Chen, 1994; Nash and Karney, 1999; V.tkovský et al., 1999, Covas et al., 2003; Kapelan et al., 2003), free-vibrational analysis (Wang et al., 2002) and also time domain reflectometry techniques (Jönsson and Larson, 1992; Brunone, 1999; Covas and Ramos, 1999). All these published fluid transient leak detection methods share a common theme in that a disturbance—a fluid transient—is injected into a pipe and the subsequent pressure response is measured and analysed to derive system information. This type of analysis is more commonly known as system response extraction and forms the basis of established methodologies used to extract dynamic responses of complex mechanical and electrical systems. The behaviour of any system can be summarized in two response diagrams, the impulse response function in the time domain and the frequency response diagram (FRD) in the frequency domain. These descriptions of system behavior are independent of the properties of the input excitation injected into the system and provide a fundamental view of the transient response from the pipeline. These response functions also allow direct comparison of transient behaviour from one day to the next without the need for a repeatable input signal.

Lee et al. (2002a, 2003, 2005a) proposed a method of leak detection where the location and size of leaks within a pipeline can be determined from the shape of the FRD. In an intact pipeline with no frequency-dependent frictional behaviour, the peaks of the FRD are of equal magnitude and equally spaced. In the case where a leak exists within the system, the magnitude of the peaks in the FRD varies in a sinusoidal-like pattern. The clear distinction between the shapes of the leaking and non-leaking FRD means that a leak can be detected within the pipe without the need to compare the results to a leak-free benchmark. Lee et al. (2003, 2005a) also derived an analytical expression that describes the influence of leaks on the peaks of the FRD and shows how frequency, phase and magnitude of the peaks can determine the location and size of a leak within the system.

This paper presents a new analytical derivation illustrating how leaks influence the peaks of the FRD in the case where the oscillating inline valve used in Lee et al. (2003, 2005a) is replaced by a side-discharge solenoid valve for generating transients. The use of such valves can result in sharper transient signals and can be applied to both symmetric and antisymmetric boundary conditions. Along with the derivation of the leak-induced impact on the FRD the best measurement position for each boundary condition configuration—defined as the generation/measurement locations that provide the greatest signal to noise ratio—is determined. A technique for modifying the original transfer matrix equations presented in Chaudhry (1987) to eliminate non-linear behavior resulting from large valve perturbations is also illustrated, with matches between method of characteristics (a non-linear solution) and the linear transfer matrix equations for different flow conditions and full valve opening/closure operations. Experiments conducted at the University of Adelaide validate the proposed technique of leak detection for both symmetric and antisymmetric boundary conditions and highlight the improved resistance to system noise displayed by the method.

2 Generation and extraction of FRD from single pipeline systems

Using small perturbations to generate transients, the pipeline can be considered as a linear system where the input to the system is related to the injected transient signal and the output is the measured head response. The relationship between the input and output provides a way to describe how the input signal is modified as it propagates through the system and is an indicator of system behaviour. For the field of leak detection, describing a pipeline system in this manner is advantageous as it provides a way of quantifying the state of the system from one day to the next even though the injected transient in these two days may not be exactly identical. Given the physical state of the system remains unchanged, the system response function will be identical for all injected signals. The frequency response function for such a system with an input (x) and an output (y) is described by

$$H(\omega) = \frac{S_{XY}(\omega)}{S_{XX}(\omega)} \tag{1}$$

where $H(\omega)$ = frequency response function, $S_{XY}(\omega)$ = Fourier transform of the cross-correlation function, R, between the input (x) and the output (y) and $S_{XX}(\omega)$ is the Fourier transform of the autocorrelation of the input (Lynn, 1982). In this paper, the output is the measured transient pressure trace from the pipeline whereas the input to a pipeline can be defined as the operation that initiated the transient. When the transient is generated by the movement of a valve connected to the system, the input should represent the movement profile of this device. Chaudhry (1970) and Mpesha et al. (2001, 2002) defined this input as the variation of the dimensionless valve-opening coefficient, τ, with time. While this definition of the system input is adequate for transient signals generated by small perturbations of an initially open valve, Lee et al. (2002b) have shown that significant non-linear error can result for inline valve movements greater than 20% of the initial valve opening. The non-linear error—a result of nonlinear orifice equations relating flow and head—manifests itself as a redistribution of energy between frequencies. That is, the frequencies contained within the input do not behave independently of each other during its propagation through the system. This definition of the system input may also lead to computational errors in the transfer matrix model when the transient signal is generated by the perturbation of an initially closed inline valve.

These problems can be overcome if the input parameter is changed from the dimensionless valve opening to the induced flow perturbation at the valve, in which case the valve no longer needs to be modelled and removes any linearity constraints on the size of perturbation imposed by the valve. The input flow perturbation may be linearly related to the head perturbation during the generation of the transient by the Joukowsky formula. For an internal point in the pipeline, the Joukowsky formula is,

$$\Delta H = \frac{a \Delta Q}{2gA} \tag{2}$$

where ΔH and ΔQ are the head and discharge perturbation from the mean state at the generation point, a = wave speed and A = area of the pipeline. The magnitude of the input discharge Frequency response method for pipeline leak detection 695 perturbation can be determined from Eq. (2) and the observed head deviation resulting from the movement of the input valve. The determination of the discharge input in this fashion is only valid if the head change substituted into Eq. (2) is the result of the valve perturbation alone. The valve movement should be fast to prevent contamination of the resultant head change by possible reflections from the system. For situations where the valve is located adjacent to a system boundary, the closure of the side-discharge valve will not be fast enough to separate the input signal from the reflection at the boundary and needs to be corrected. Transients generated by rapid valve manoeuvres also minimize the error from line packing when applying Eq. (2) and have advantages in term of input signal bandwidth (described later in the paper). In the case where the side-discharge valve is located adjacent to a closed boundary with the valve perturbing in a pulse fashion, the ΔQ determined from Eq. (2) needs to be divided by 2 to represent the effective doubling of the head rise from the reflection off the closed boundary. Another advantage of this choice of the input signal is that the valve movement profile does not need to be measured; instead, the input signal can be determined directly from the observed perturbation of the head (the measured output). Each transient response can, therefore, be considered as consisting of two parts, the part directly associated with the movement of the input device and the response from the pipeline system resulting from the injected signal. An alternative to using Eq. (2) that may be useful in field situations is to analyse the initial pressure output during the valve closure using the method of characteristics to generate the corresponding flow variation history.

A similar selection of the input signal was also shown in Suo and Wylie (1989) and Ferrante et al. (2001). These papers propose a transfer function in the form of a ratio between the measured head and discharge perturbation for the entire duration of the transient signal. The application of this approach is limited to cases where the actual discharge perturbation at the valve is measured or can be assumed to be a result of the valve manoeuvre alone. For example, in cases where an inline valve was not fully closed after the manoeuvre, a point upstream of the valve will have discharge perturbations throughout the duration of the transient (due to pressure fluctuations) and these perturbations need to be taken into account.

An input defined as the discharge variation at the valve is also incompatible with the system structure assumed in Eq. (1). The use of Eq. (1) assumes the input signal is independent of the behaviour of the output, that is, the magnitude of the response from the system does not affect the shape or form of the input signal (Lynn, 1982). If the valve is not fully closed after generation of a transient, the discharge perturbation at the valve after the arrival of the first reflection from the system is a function of the measured head response and a feedback loop is established in the system. For an accurate description of the system response in such a situation the feedback loop must be taken into account. In this paper, the input to the system is described as the discharge change induced by the valve motion and this input is assumed to be independent of the measured head response (the output).

In addition to the correct selection of input and output parameters, the location of the transient source and measurement transducers also play important roles in the extraction of the FRD. Lee et al. (2005b) have defined the optimum measurement position for an antisymmetric system, which is at the system boundary. In this paper, all transients are generated by the perturbation of a side-discharge valve, which has the advantage of generating fast, small amplitude transients that induce minimal impact on the base flow through the system. Such devices can be easily connected to existing pipelines for the application of the leak detection method.

The use of a side-discharge device means that the optimum extraction of the FRD will depend on the position of both the measurement transducer and the side-discharge valve for all possible boundary conditions. For a single pipeline, two possible boundary configurations are considered:

- Open–open boundary (symmetric)—a pipeline bounded by reservoirs on each end with hydraulic elements (e.g. joints, inline valves) along its length that have small impedances relative to the overall pipe impedance.
- Open–closed boundary (antisymmetric)—a pipeline bounded by an upstream reservoir and a high impedance device on the downstream end that can be a high loss or fully closed valve. Note that the term "closed" boundary does not only imply a fully closed valve, but can also be used to describe any boundary condition where the impedance of the boundary device is greater than that of the entire pipeline.

The optimum arrangement of the measurement and generation positions in a single pipeline for both configuration types is illustrated in the following investigation. A 0.3-m diameter intact pipeline has a reservoir with 50m head at the upstream end and a downstream reservoir with 20m head. The length and wave speed of the pipeline are 2000m and 1200ms^{-1} respectively. In the antisymmetric case, a static and fully open inline valve with a loss coefficient, C_v, of 0.02m$^{5/2}$s^{-1} is located at the downstream boundary. Figures 1 and 2 show the variation of the frequency response magnitude as the measuring point is shifted along the pipeline for the symmetric and antisymmetric system respectively. Each series in the figures corresponds to a different location of the side-discharge excitation valve. The magnitude of the response for the peaks of the FRD are averaged over the first 1024 peaks and the positions of maximum response indicate locations in the pipe where the best signal to noise ratio can be achieved. In Fig. 1, the maximum response is located at the centre of the pipeline for all positions of the transient source and the maximum signal to noise ratio occurs if both the transient generation and the measurement occur at the centre of the pipe. Following the same argument, the optimum location for both the generation and measurement in the antisymmetric pipeline is adjacent to the closed boundary in Fig. 2.

The procedure for extracting an accurate FRD from a single pipeline system is as follows:

1. Place the measurement transducer and side-discharge valve at the midpoint of the pipeline for a symmetric system and adjacent to the closed boundary for an antisymmetric system.
2. Generate a short-duration transient event (e.g. a pulse) and measure the head response at the generation point until the signal has fully attenuated. Identify the portion of the transient directly related to the movement of the side-discharge valve. This is the input signal.
3. Using Eq. (2) and the injected-head perturbation, determine the corresponding discharge perturbation caused by the valve movement. For an antisymmetric system divide the righthand side of Eq. (2) by 2 to compensate for the doubling in the measured-head response due to the reflection off the closed valve during generation. This is the input to the system.

4. Using the entire measured-head perturbation response as the output, apply Eq. (1) to obtain the FRD of the pipeline system.
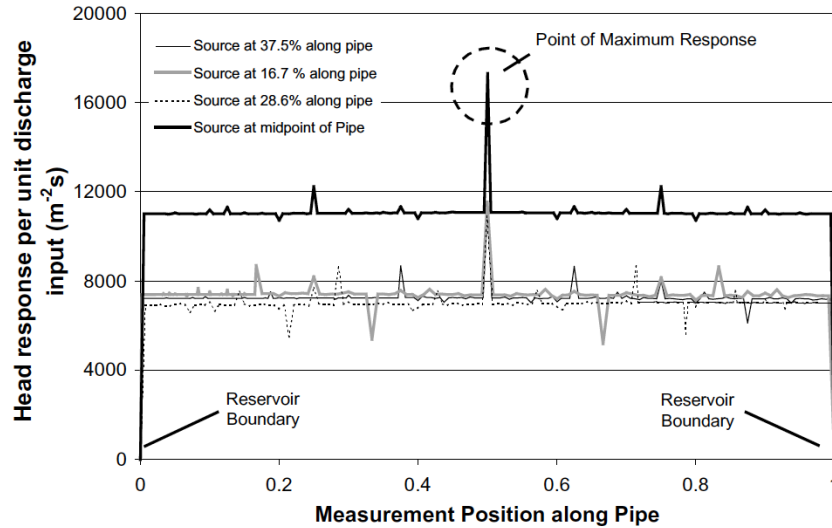

Figure 1: Average response magnitude for varying measurement and generation position for a symmetric system.
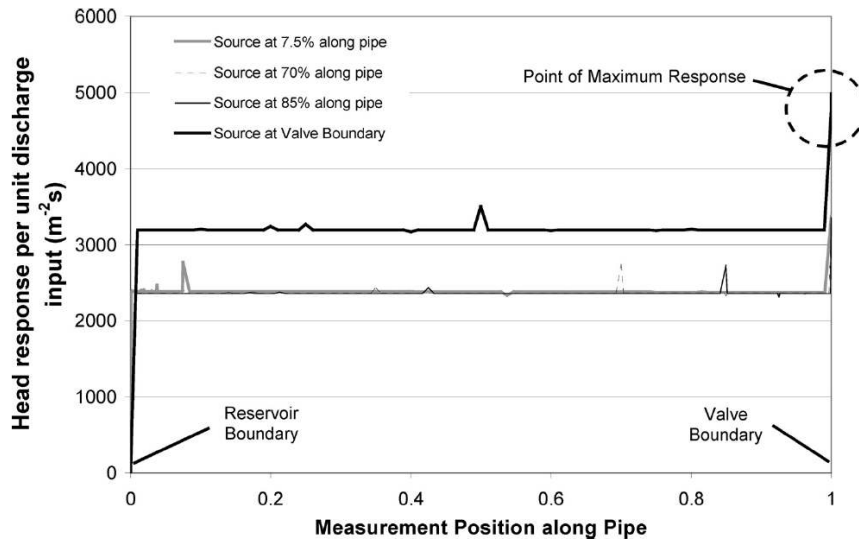

Figure 2: Average response magnitude for varying measurement and generation position for an antisymmetric system.

Figures 3 and 4 show the numerical comparison between the FRD produced from the above procedure and those generated from the transfer matrix method (Chaudhry, 1987) for the 0.3-m diameter pipeline system used in Figs 1 and 2. The time series traces are generated using the method of characteristics and the transient is initiated by a single pulse perturbation of an initially closed side-discharge valve. Excellent matches are produced between the linear transfer matrix method and the non-linear method of characteristics (MOC) model, even though the largest possible perturbation (closed to fully open to closed) was used. The proposed method for FRD extraction is shown to avoid the substantial non-linearity errors presented in Lee et al. (2002b) for large inline valve perturbations.

3 Derivation of the leak-induced impact

Previous publications on steady oscillatory flow in single pipelines have indicated that for an intact system with no frequency-dependent frictional behaviour, the peaks of the FRD are equal in magnitude and are equally spaced as illustrated in Figs 3 and 4. Similar results are shown in Ferrante et al. (2001). In the case where a leak exists within the system, the peaks of the FRD undergo changes where the magnitude of the peaks vary in a sinusoidal-like pattern as shown in Fig. 5. This figure shows the FRD from the system of Fig. 4 with a leak located at 1400m from the upstream boundary compared to the FRD of the no-leak pipe. As illustrated by Fig. 5, the shape of the FRD for the leaking pipe is significantly

different from that of the intact system. Therefore, the integrity of pipeline system can be ascertained by identifying periodic patterns within the peaks of the FRD. This method represents a significant advantage to leak detection as it removes the need for a "leak-free" benchmark for comparison or an accurate transient model.

Figure 3: Comparison between FRD generated from the transfer matrix equation and the proposed technique using time series results from method of characteristics for a symmetric system.
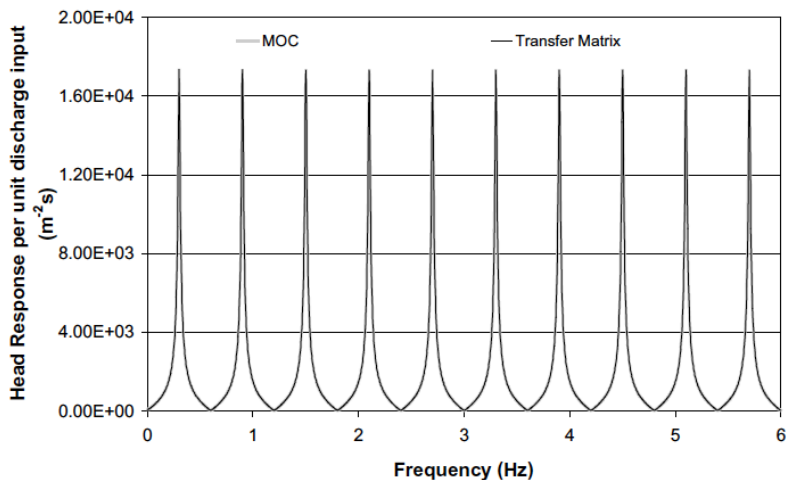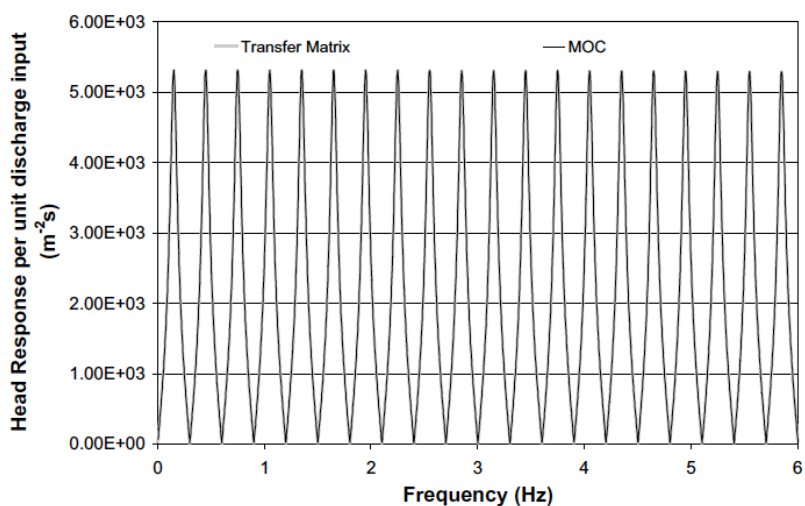
Figure 4: Comparison between FRD generated from the transfer matrix equations and the proposed technique using time series results from method of characteristics for an antisymmetric system.
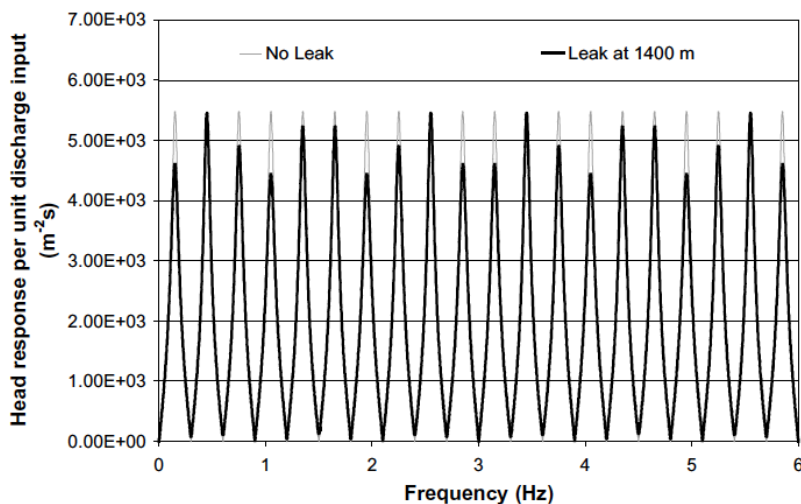
Figure 5: FRD of a leaking and non-leaking pipeline.

Lee et al. (2003) have derived an analytical expression for the observed leak-induced impact for an antisymmetric system consisting of an inline excitation valve at an extremity of the system. The frequency and phase of the leak-induced effect on the FRD can be used to determine the leak location, whereas the magnitude of the effect on the FRD can be used to find the leak size. In this section, the analytical expression that describes the leak-induced pattern on the FRD is derived for transients generated by a side discharge valve for both symmetric and antisymmetric boundary conditions.

3.1 Symmetric system

Consider first a simple symmetric system where a side-discharge valve is located at the midpoint of the pipe, and a leak exists somewhere within the system as shown in Fig. 6. Each element of the pipeline can be described by a set of linearized equations that represent a transfer between the upstream and downstream head and discharge perturbations. For ease of computation these equations are placed in matrix form. These matrices, representing different hydraulic elements, are multiplied together starting from the downstream end to produce the overall transfer matrix for the entire system. Details of the derivation and use of the transfer matrix method can be found in Chaudhry (1987). To isolate the effect of a leak on the peaks of the FRD, the intact pipe segments are modelled as frictionless units with the field matrix given as

$$\begin{Bmatrix} q \\ h \end{Bmatrix}^{n+1} = \begin{bmatrix} \cos\left(\dfrac{l\omega}{a}\right) & -\dfrac{igA}{a}\sin\left(\dfrac{l\omega}{a}\right) \\ -\dfrac{ia}{gA}\sin\left(\dfrac{l\omega}{a}\right) & \cos\left(\dfrac{l\omega}{a}\right) \end{bmatrix} \begin{Bmatrix} q \\ h \end{Bmatrix}^{n} \tag{3}$$

where q, h = complex discharge and head at either end of the pipe section and l = the length of the section. The superscripts n and n+1 indicate positions in the system upstream and downstream of the pipe respectively, and ω is the angular frequency. The leak matrix is

$$\begin{Bmatrix} q \\ h \end{Bmatrix}^{n+1} = \begin{bmatrix} 1 & -\dfrac{Q_{LO}}{2H_{LO}} \\ 0 & 1 \end{bmatrix} \begin{Bmatrix} q \\ h \end{Bmatrix}^{n} \tag{4}$$

where Q_{L0} and H_{L0} are the steady-state discharge and head at the leak. As the discharge perturbation is used as the input to the system, the transient source can be modelled as a point where a unit discharge perturbation takes place,

$$\begin{Bmatrix} q \\ h \end{Bmatrix}^{n+1} = \begin{bmatrix} 1 & 0 \\ 0 & 1 \end{bmatrix} \begin{Bmatrix} q \\ h \end{Bmatrix}^{n} + \begin{bmatrix} 1 \\ 0 \end{bmatrix} \tag{5}$$
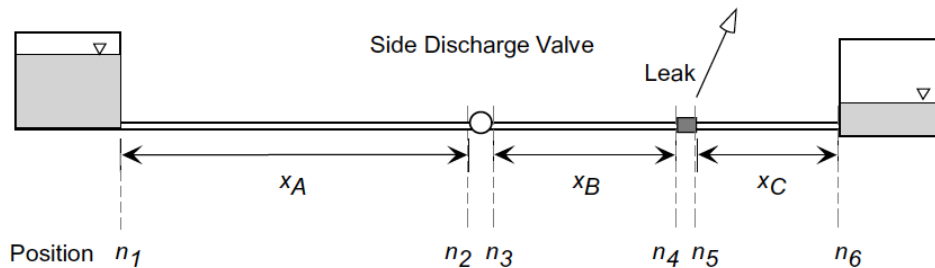
Figure 6: System configuration for the derivation of the leak impact in an symmetric boundary.

The overall transfer matrix of the entire system is formed by multiplying the matrices of all the elements within the system, starting from the downstream end, and is given as

$$\begin{Bmatrix} q \\ h \\ i \end{Bmatrix}^{n_6} = \begin{bmatrix} U_{11} & U_{12} & U_{13} \\ U_{21} & U_{22} & U_{23} \\ U_{31} & U_{32} & U_{33} \end{bmatrix} \begin{Bmatrix} q \\ h \\ i \end{Bmatrix}^{n_1} \tag{6}$$

where U_{jk} = j^{th} row and k^{th} column entry for the overall transfer matrix for the pipeline system and n_1, n_6 are points denoting the upstream and downstream boundaries of the pipe as shown in Fig. 6. An

additional third row and column is needed in Eq. (6) to cater for the unit discharge perturbation imposed on to the system through Eq. (5). Expanding Eq. (6) gives

$$q_{n_6} = U_{11}q_{n_1} + U_{12}h_{n_1} + U_{13}$$
$$h_{n_6} = U_{21}q_{n_1} + U_{22}h_{n_1} + U_{23}$$

(7)

By substituting the reservoir boundary conditions ($h_{n_1}, h_{n_6} = 0$), Eq. (8) can be used to solve for the discharge perturbations at the upstream boundary,

$$q_{n_1} = \frac{-U_{23}}{U_{21}}$$

(8)

Given that the transient source is at the optimum measurement position, the magnitude of the head perturbation at the transient generating point is determined by substituting the upstream boundary head and discharge perturbation into the field matrix of pipe section A as indicated in Fig. 6. Solving the resultant equation and simplifying gives

$$h_{n_2} = h_{n_3}$$

$$= \frac{1 + (-1)^m \frac{iQ_{L0}a}{4H_{L0}gA}[\cos(x_B^* - x_C^*(2m-1)\pi)]}{\frac{Q_{L0}a}{4H_{L0}gA}((-1)^{m+1} + (-1)^m \cos[4\pi m(x_A^* + x_B^*) - 2\pi(x_A^* + x_B^*)])}$$

(9)

where x_i^* = ratio of the length of the ith pipe section to the total length of the pipeline. The parameter m denotes the peak number in the FRD. Note that x_A^* is known (the position of the transient source) while x_B^* and x_C^* are unknowns.

To further simply the equation, the term $(Q_{L0}a)/(4H_{L0}gA)$ in the numerator of Eq. (10) can be shown to be negligible for reasonable leak sizes. For a wave speed equal to 1200 ms^{-1} and dimensionless leak sizes less than 0.002 of the pipe cross-sectional area and head at the leak greater than 50 m, $(Q_{L0}a)/(4H_{L0}gA) \ll 1$, therefore, under realistic combinations of leak size and driving head this term can be neglected. Using this result and defining the dimensionless distance of the leak from the upstream boundary $(x_A^* + x_B^*)$ as x_L^*, the inverted and absolute value of Eq. (10) is

$$\frac{1}{|h_{n_2}|} = \frac{Q_{L0}}{4H_{L0}}(1 - \cos(4\pi m x_L^* - 2\pi x_L^*))$$

(10)

Equation (11) indicates that the presence of a leak in the pipeline results in a sinusoidal function being imposed on the inverted magnitude of the harmonic peaks in the FRD. Note that due to the symmetry of the system, a leak located at the mirror position of the pipeline will have the same effect on the frequency response function.

3.2 Antisymmetric system

A similar equation can be derived for an antisymmetric system, with a valve forming a high impedance boundary on the downstream end, as illustrated in Fig. 7. The side-discharge valve is now located adjacent the closed boundary, which is the optimal generation/measurement position shown in Fig. 2. To solve this system, the overall transfer matrix is reformulated to include the inline valve. The discharge perturbation at the downstream reservoir, q_{n_6}, can be determined using Eqs (7) and (8) and the boundary conditions, $h_{n_1}, h_{n_6} = 0$. The transfer matrix for the inline valve is

$$\begin{Bmatrix} q \\ h \end{Bmatrix}^{n_6} = \begin{bmatrix} 1 & 0 \\ -\dfrac{2\Delta H_{VO}}{Q_{VO}} & 1 \end{bmatrix} \begin{Bmatrix} q \\ h \end{Bmatrix}^{n_5}$$

(11)

where ΔH_{V0}, Q_{V0} = the steady-state head loss across and flow through the valve, respectively. The

magnitude of the inverted head perturbation upstream of the valve is

$$\frac{1}{|h_{n_5}|} = \frac{Q_{LO}}{4H_{LO}}(1 - \cos(2\pi m x_L^* - \pi x_L^*)) + \frac{Q_{VO}}{2\Delta H_{VO}} \qquad (12)$$
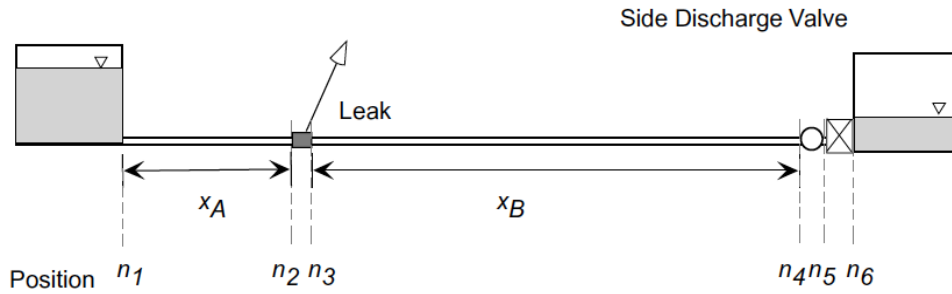

Figure 7: System configuration for the derivation of the leak impact in an antisymmetric boundary.

Equations (11) and (13) indicate that the oscillation frequency of the peak magnitudes (given by the coefficient of m in the cosine functions) is a measure of the leak distance from a reservoir boundary. Specifically, for a symmetric case, the frequency of oscillation is twice the dimensionless distance of the leak from a reservoir boundary ($2x_L^*$), whereas it is equal to the leak distance for the antisymmetric case (x_L^*). The observed frequency of oscillation, however, will never exceed 0.5 because of the sampling theorem. The frequency of 0.5 is the maximum observable frequency when sampling the sinusoidal function at every peak value, as shown in Eqs (11) and (13). This maximum frequency is the Nyquist frequency, defined as half the sampling frequency. Any frequency of oscillation higher than this value will be aliased down to a lower frequency in the range of 0 and 0.5 given by

$$\omega'_{signal} = 2\omega_{nq} - \omega_{signal} \qquad (13)$$

where ω'_{signal} and ω_{signal} are the distorted and the original signal frequencies, and ω_{nq} is the Nyquist frequency. Thus, an observed frequency of oscillation in the peak may be due to two different leak positions, one associated with an oscillation below the Nyquist frequency and one above. To identify the true leak position, the phase of the oscillation is used. Ambardar (1999) stated that for down-aliased signals, where $\omega_{signal} < 2\omega_{nq}$ the phase of the original signal undergoes a reversal.

$$\phi'_{signal} = -\phi_{signal} \qquad (14)$$

This result can be used to divide the unit circle into two zones, where each zone is associated with a different region within the pipeline. The phase of the leak-induced oscillation can thus be used to find which zone the signal falls into, and is translated into a region of the pipe using Fig. 8. Note that the zones within the unit circle in Fig. 8 have been expanded from the original quadrants indicated in Eqs (11) and (13) to allow for possible uncertainty in the phase data.
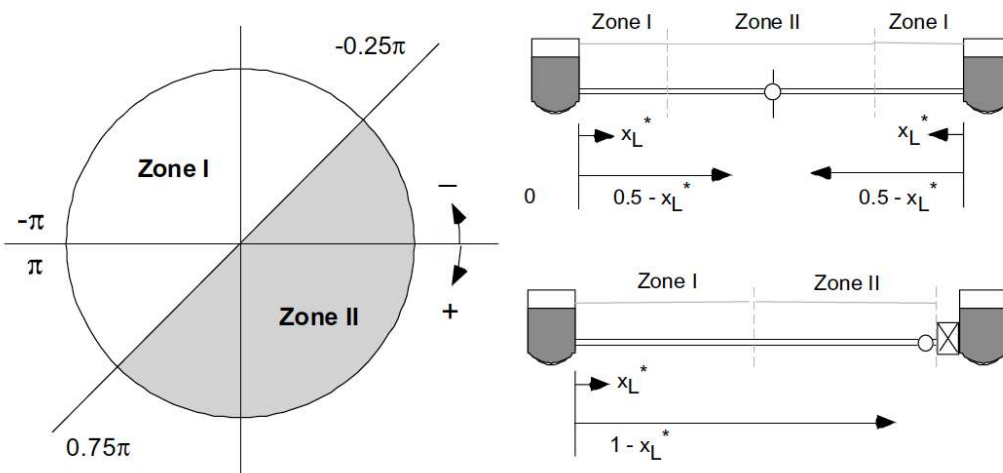

Figure 8: Phase zones to identify leak location.

For the symmetric system configuration, the sinusoidal oscillation imposed on the peaks of the FRD has the following properties as shown in Eq. (11):

- The frequency of the leak-induced damping pattern is $2x_L^*$ for $x_L^* < 0.25$, and $1 - 2x_L^*$ for $0.5 > x_L^* > 0.25$. Due to the symmetry of the system for $x_L^* > 0.5$, the results are identical to that when $x_L^* = 1 - x_L^*$.
- The phase of the leak-induced damping pattern is $\pm\pi$ $(1 + x_L^*)$ and the phase is located in zone I when $x_L^* < 0.25$, $x_L^* > 0.75$ and in zone II when $0.75 > x_L^* > 0.25$.
- The magnitude of the leak-induced damping pattern is $Q_{L0}/(4H_{L0})$.

For an antisymmetric system:
- The frequency of the leak-induced damping pattern is x_L^* for $x_L^* < 0.5$ or $1 - x_L^*$ for $x_L^* > 0.5$.
- The phase of the leak-induced damping pattern is $\pm\pi$ $(1 + x_L^*)$ and the phase is located in zone I when $x_L^* < 0.5$ and in zone II when $x_L^* > 0.5$.
- The magnitude of the leak-induced damping pattern is $Q_{L0}/(4H_{L0})$.

Note that the sinusoidal impact is imposed on the inverted peak magnitudes and the accurate extraction of this oscillation requires the inversion of the FRD peak responses. The following section explains how the proposed method can be used for leak location in an experimental single pipeline.

4 Leak detection procedure

The study is carried out on an experimental pipeline at the University of Adelaide. The system comprises a 0.022-m diameter copper pipe of a total length of 37.53m and five brass blocks spaced along its length for the connection of side-discharge valves and pressure transducers. These brass blocks are machined with an internal bore that connects smoothly to adjacent pipe sections. The pipe slope is constant throughout with a vertical to horizontal ratio of 1V:18.5H. The elevation difference between the two ends of the pipe is 2m. The pressure transducers are flush-fitted Druck PDCR 810 with a rise time of 5µs. The data acquisition card has a maximum sampling rate of 100 kHz and pressures are sampled at a frequency of 2000 Hz. To ensure minimal pipe vibration, wall-mounted supports are located at every 0.4m along its length. The wave speed of the pipeline has been experimentally determined to be 1328ms^{-1}. The schematic of the system is shown in Fig. 9. A side-discharge brass solenoid valve mounted on the brass blocks is used to carry out the generation of the transient and is electronically controlled to open and close in the time of 4 ms, injecting a sharp pulse into the system. The dimensionless valve coefficient $C_d A_V/A$ is 4.6 x 10^{-3}, where C_d is the coefficient of discharge, A_V is the area of the valve and A is the area of the pipe.
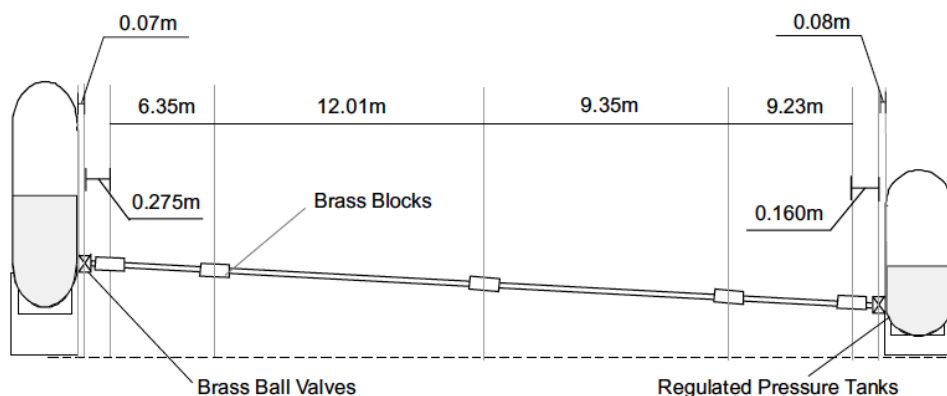
Figure 9: Schematic of experimental pipeline at the University of Adelaide.

In the previous section, the leak-induced impacts on the FRD for both symmetric and antisymmetric boundary conditions were derived. In a physical system the oscillation frequency and phase of leak-induced oscillation are dependent on the input signal bandwidth and pipe frequency-dependent behaviour.

4.1 Impact of input signal bandwidth

The frequency and phase of the oscillation pattern on the peaks of the FRD determines the leak position.

While theoretically these parameters can be found using a fast Fourier transform of the inverted peak magnitudes, in reality the number of peaks that can be observed in the FRD is limited by the bandwidth of the injected signal and the amount of noise prevalent in the system. The concept of signal bandwidth is best described as the amount of frequency information contained within the input signal. When a signal is injected into a system, the amount of information that is contained within the output is bounded by the bandwidth of the injected signal. For example, if an input signal with frequency content ranging from 0 to 50Hz was injected into the system, the frequency content of the output response would also be between 0 and 50 Hz, and any detected response outside this range is a result of system noise alone. For best accuracy, therefore, the determination of the system integrity should only be carried out in the frequency range within the bandwidth of the injected signal (0–50 Hz). The valve movement used to generate the transient signal should be fast to maximize the information content of the measured response from the pipeline. The use of slow pump trips or manual closures of side-discharge valves will generate transient signals of low information content (frequency range) and such signals are not ideal for leak detection.

Figure 10 shows the spectrum for a typical pressure pulse generated in the experimental pipeline with a width of 4 ms. For this paper, the bandwidth of the input signal is defined as the frequency where the magnitude of the input signal spectrum falls below 5% of its maximum value. For different pipeline systems this setting may vary depending on the level of background noise and is the point on the frequency axis beyond which crisp peaks in the FRD can no longer be observed. From Fig. 10 the bandwidth is 300 Hz. Given that the fundamental frequency in the symmetric experimental pipe is 17.7 Hz and for the antisymmetric case is 8.8 Hz, a bandwidth of 300 Hz will produce eight peaks for the symmetric configuration and 16 peaks for the antisymmetric case. A Fourier transform performed on this low number of data creates a spectrum that can only locate a leak to an accuracy of 6.25% of the total pipe length and is only acceptable as an initial estimate. To produce an accurate assessment of the oscillation frequency and phase, a shuffled complex evolution (SCE) algorithm is used to fit a cosine function to the data series. The resultant frequency and phase of the best-fit cosine function are converted into a predicted leak location using Eqs (11) and (13).
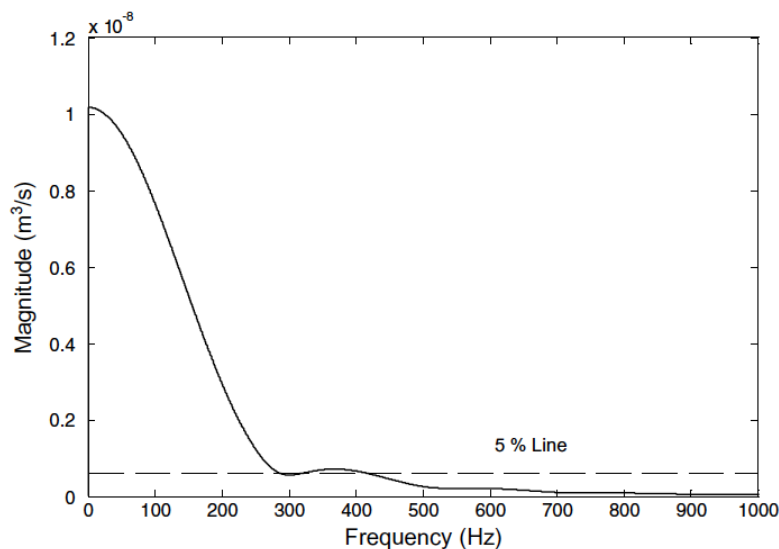

Figure 10: Spectrum of an input discharge pulse.

4.2 Impact of other frequency-dependent behaviour

Equations (11) and (13) illustrate the effect of a leak on the peaks of the FRD in a single pipeline system. The effects of other frequency-dependent behaviour is superimposed onto these results in real experimental data and must be taken into account. Frequency-dependent behaviour can be associated with unsteady friction, pipe viscoelastic effects and also physical non-uniformities in the system. While steady friction produces a frequency-independent effect bringing about a uniform reduction in peak magnitudes across the frequencies, unsteady friction induces a non-linear trend in the peaks of the FRD (Vitkovský et al., 2003). Viscoelastic behaviour and physical imperfections in the system can also result in similar systematic distortions of the leak-induced oscillations. Systematic distortions of the leak-induced oscillation can occur in two forms:

1. Trend distortion—where the mean of the leak-induced oscillation shifts with frequency. Figure 11 shows an example of trend distortion where the mean of the oscillation increases non-linearly.

2. Scale distortion—where the magnitude of the leak-induced oscillation changes with frequency and is a result of magnitude-dependent attenuation in the peaks of the FRD. The nature of this type of distortion is shown in Fig. 12.
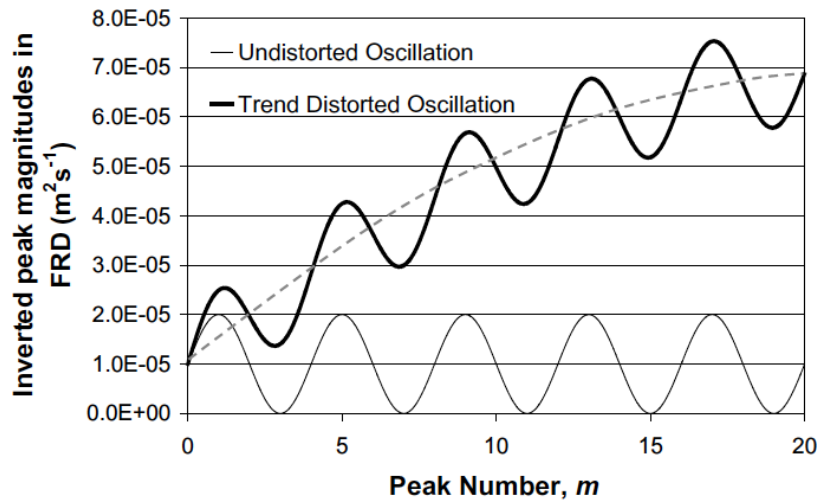

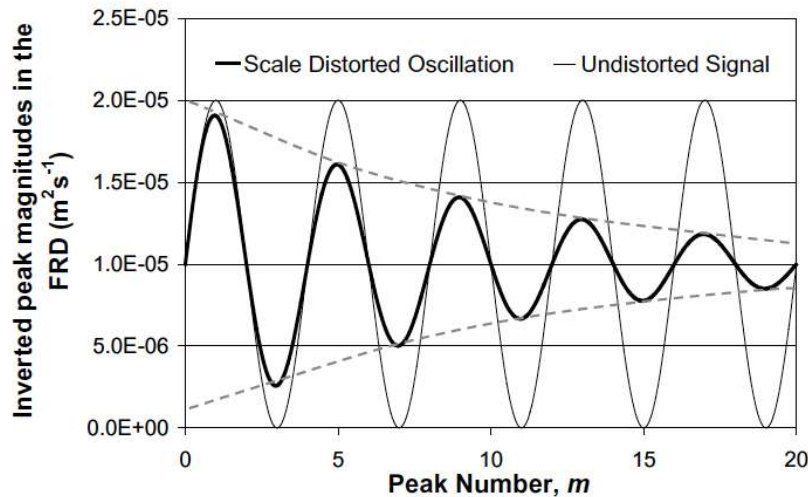Figure 11: Trend distortion effects on the peak oscillations as a result of unsteady friction.

Figure 12: Scale distortion effects on the peak oscillations.

To provide an accurate and flexible leak-induced oscillation extraction procedure, both of these distortions need to be considered. Conventional fast Fourier transform algorithms cannot describe signals with components where the period is greater than the data length (e.g. trends) and a customized procedure is required for situations where systematic scale and trend distortions exist within the data. It is proposed that a least squares regression of a scale- and trend-corrected sinusoid fitted to the inverted peak data points can give the dominant oscillation frequency while taking into account the trend and scaling of frequency-dependent effects. The fitting function is of the form,

$$F(m) = \frac{1}{S(m)} \times X_1 \cos(2\pi m X_2 - X_3) + T(m)$$

(15)

where, X_1 are the fitted parameters and m is the resonant peak number as defined previously. The parameters X_2 and X_3 are the frequency and phase of the oscillation, which are used to determine the location of the leak within the pipe. The functions T and S are the trend- and scale-correction functions respectively. The form of the scale- and trend-correction functions must be flexible to permit a wide range of possible distortions in the leak induced oscillations.

Systematic trend distortion is predominantly the result of unsteady friction effects within the pipe (Vitkovský et al., 2003). It is valid, therefore, to base the form of the trend-correction function in Eq. (16) on the influence of unsteady friction on the FRD. Figure 13 shows the impact of unsteady friction on the inverted peaks of the FRD for both laminar and turbulent flow. The Reynolds numbers for the examples shown are 30 and 44,900 respectively. This trend in the peaks of the FRD is approximated as a power law function of the form

$$T(m) = X_4 m^{X_5} + X_6 m + X_7 \tag{16}$$

and was shown to provide a good match with the unsteady friction behaviour in Fig. 13.
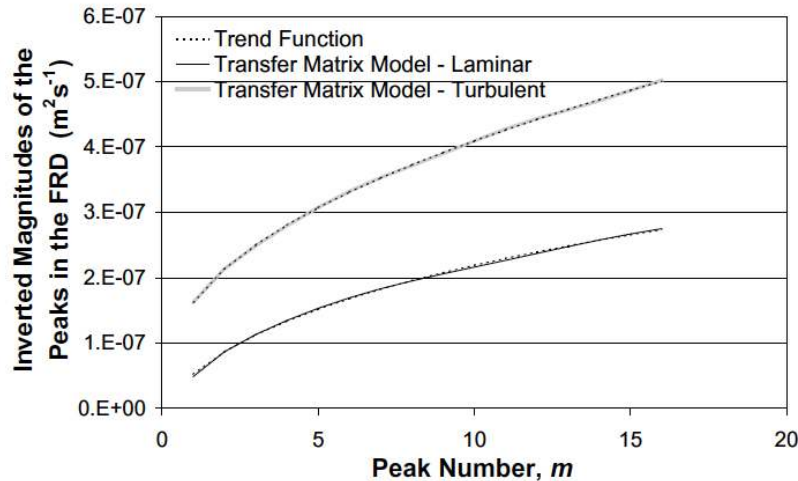

Figure 13: The comparison between the trend correction function for laminar and turbulent flow cases.

Unlike trend distortion, the presence of systematic scale distortions in the oscillation cannot be attributed to a single phenomenon within a pipeline system. The extent of this distortion is dependent on the nature of the system under consideration. The cause of this type of damping can be a result of pipe non-uniformity due to the presence of transducer blocks, fluid structure interaction or structural vibration. To allow for all possible magnitudes of this distortion, the scale correction is given as a generic power logarithmic function,

$$S(m) = X_8 (\ln(m))^{X_9} + X_{10} + 1 \tag{17}$$

The SCE algorithm is used to fit Eq. (16) to the inverted peak magnitudes obtained from the experimental results, giving the dominant oscillation frequency in the data (hence location of the leak). It is not necessary to model the physical behaviour of the system in order to extract the oscillation parameters from the FRD peaks. Traditional transient leak detection requires the accurate determination of system parameters such as friction factors and valve loss coefficients. The proposed technique requires the accurate extraction of the periodic oscillation in the peaks of the FRD and the baseline about which this oscillation takes place— given by the absolute magnitude of the FRD—is not important. Note that the technique is also insensitive to the estimation of system wave speed. A change in the wave speed will alter the position of the resonance peaks on the frequency axis, but will not affect the relative sizes of the peaks and the accuracy of the approach.

Although the leak size is related to the amplitude of the leak induced pattern on the FRD (Lee et al., 2003), the true amplitude of the pattern cannot be separated from the scale correction function, S(m), in Eq. (16). Hence a good knowledge of the frequency-dependent behaviour of the system is required for an accurate prediction of the leak size. For a system with unknown characteristics, this prior knowledge of the system behavior is not easily obtained and the predicted leak size will not be accurate.

The limited number of available peaks introduces an additional complication that applies to the validation of the procedure under laboratory conditions. In such cases, the length of the pipeline is short, giving a large fundamental frequency of the system. For a signal of finite bandwidth, the number of available data points can be less than the number of fitted parameters, giving an underdetermined system for the regression process. The accuracy of the fitted parameters should therefore be ascertained through the

parameter variance, where a small value indicates that the parameter is well determined. The parameter variance is found from the diagonal entries of the covariance matrix formed in the regression process. Parameter correlations from the off-diagonal entries in the covariance matrix should also be used to ensure that the leak parameters (X_2, X_3) are independent of other parameters.

The procedure for detecting and locating leaks using the FRD is as follows:

1. Extract the pipeline FRD as described previously.
2. Isolate peak responses from the FRD and invert the responses.
3. Use the SCE to perform a least squares regression of Eq. (16) to the inverted peak responses. Find the dominant frequency and phase of the oscillation.
4. Use the frequency and phase to find the location of the leak using the results of Eqs (11) and (13), and Fig. 8.

5 Experimental verification

A series of experimental tests have been conducted for both boundary condition configurations to validate the technique proposed in this paper.

5.1 Symmetric system

The symmetric system tests were carried out in the experimental pipe by opening all inline valves in the system and setting the boundary pressures as 38.5 and 37.0 m. The flow velocity was 0.5ms^{-1} giving a Reynolds number of 11,000. The transient was generated by the side-discharge valve located close to the midpoint of the system (18.705m from one boundary). The test case contains a leak located 6.695m from the upstream reservoir boundary of a dimensionless leak size, $C_dA_L/A = 4.6 \times 10^{-3}$. The elevation at the leak is 1.64 m. The resultant transient was measured at the transient source and the input and output time series are shown in Fig. 14. The input to the system is determined from the head perturbation at the side-discharge valve. Using the input and output, the FRD of the system is extracted using Eq. (1) and is displayed in Fig. 15.
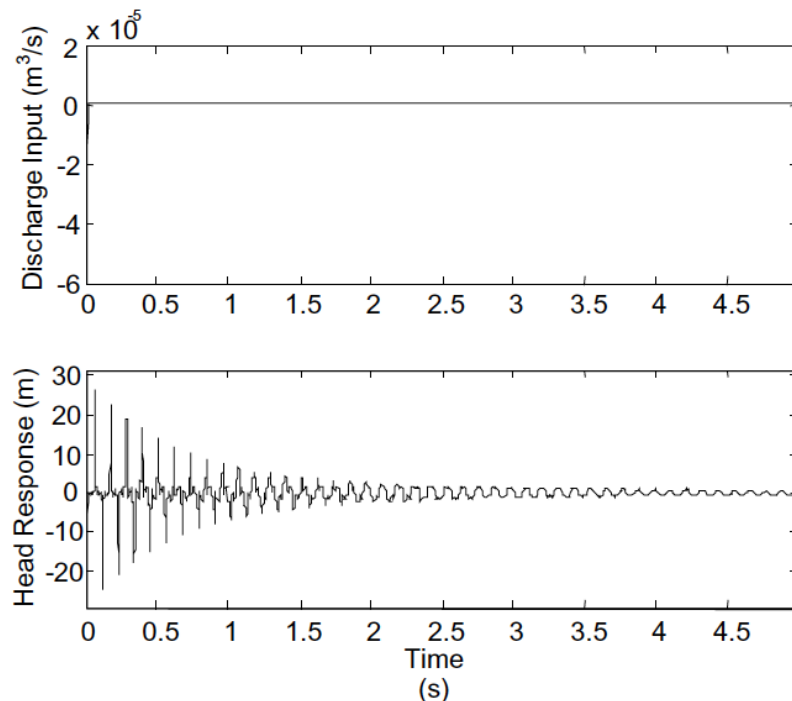

Figure 14: Time series of the input and output signal for symmetric case with leak located at 6.695m away from reservoir boundary.

From Fig. 15, the peaks of the FRD vary non-uniformly, indicating that a leak exists somewhere within the pipe. The function of Eq. (16) is fitted to the inverted peak magnitudes to determine the dominant oscillation frequency and phase of the peak magnitudes. Due to the low number of data points, the search space is divided into subsections, and the least squares fit for each subsection is found. The best

solution out of these is the optimum solution for the entire search space. The search space is divided based on the parameter, X_2, the oscillation frequency. A search is conducted within five possible ranges for X_2, with bounds for the first section as $0 \leq X_2 \leq 0.1$, $0.1 \leq X_2 \leq 0.2$ for the next and so forth up to the maximum of 0.5. The bounds for the phase of the oscillation (X_3) are set between $-\pi$ to $+\pi$ while all other parameters are unbounded for each of these runs.
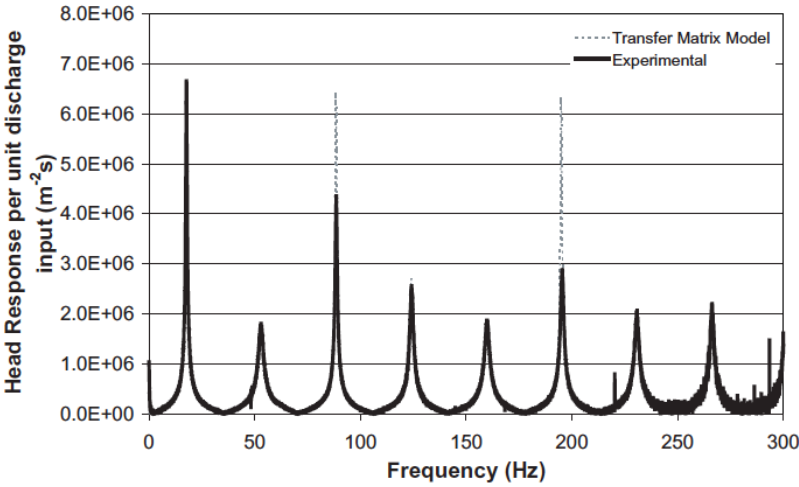

Figure 15 Experimentally derived frequency response diagram for symmetric system with leak located at 6.695 m from reservoir boundary.

Figure 16 shows the match between the SCE regression and Eq. (16). The resultant frequency was found to be $1/m = 0.358 \pm 0.03$. This frequency of oscillation indicates that a leak can be located in four possible positions in this symmetric system: $x_L^* = 0.179, 0.321, 0.679$ or 0.821 all with an error of 0.015. The mean phase of the oscillation was found to be -2.069 rads, and according to Fig. 8, place the results within zone I of the pipeline. The leak is, therefore, predicted at a position $x_L^* = 0.179 \pm 0.015$ from one of the reservoir boundaries, which corresponds to a distance of 6.71 ± 0.56 m. The predicted result is in agreement with the true leak position of 6.695m from a reservoir boundary. Note that due to the low number of data points (giving an underdetermined system), the variances for some other parameters within the fit are poor. However, the fitting of these parameters has little impact on the accuracy of the predicted leak location and is illustrated in the correlation matrix formed from the fitting procedure. The correlation of the variable X_2 with other variables $[X_1, X_3, \ldots, X_{10}]$ are given as $[-0.00113, 0.927, 0.0190, -0.0788, 0.257, -0.0169, -0.0435, 0.581, 0.0127]$ respectively. From the correlation matrix, strong correlation is only observed between the oscillation frequency and phase, and not with other fitted parameters.
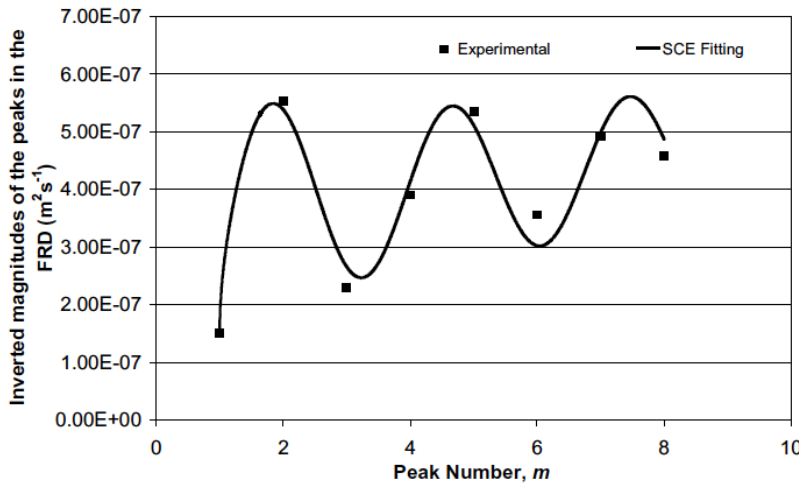

Figure 16: Dominant frequency extraction in inverted frequency response diagram peaks for symmetric system with leak located 6.695m from upstream boundary.

5.2 Antisymmetric system

The experimental pipeline was turned into an antisymmetric system by closing the inline valve on the downstream end of the pipe. The transient source and measurement transducer were relocated to this closed boundary as indicated in Fig. 2. A leak is placed at a position 9.39m upstream of the closed boundary at an elevation of 0.5 m. The experimental FRD extracted from the system is shown in Fig. 17. The FRD from the pipeline displays a periodic pattern in the peaks, indicating that a leak exists within the system. The inverted peaks of the FRD are shown in Fig. 18. Using the SCE algorithm to fit to the inverted peaks of this FRD gives the frequency of the signal as 0.244 ± 0.008 and the mean phase as 0.215. The phase result places the leak within zone II of the pipeline and the frequency indicates that the leak is located at a position 9.586 ± 0.3m upstream of the closed valve. This result is again in agreement with the true leak position of 9.39m upstream of the valve. Note that in both boundary configurations, the parameter variance of the oscillation frequency is small, indicating that the leak position is well found.
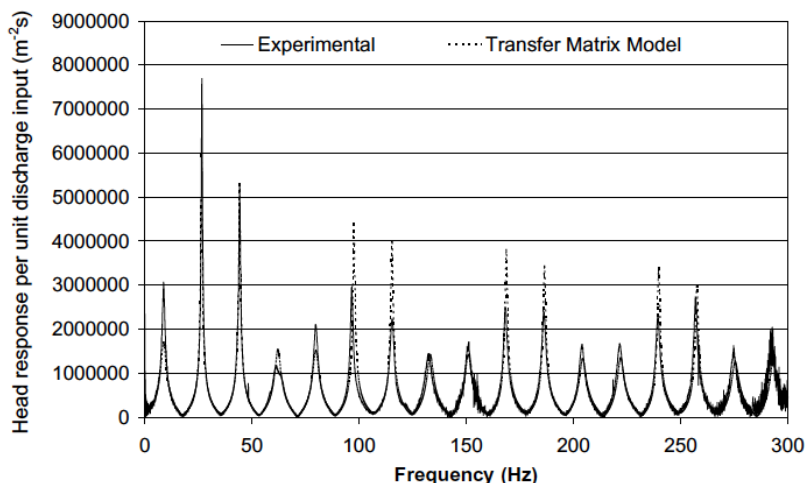

Figure 17: Experimentally derived frequency response diagram for antisymmetric system with leak located at 9.39m from closed boundary.
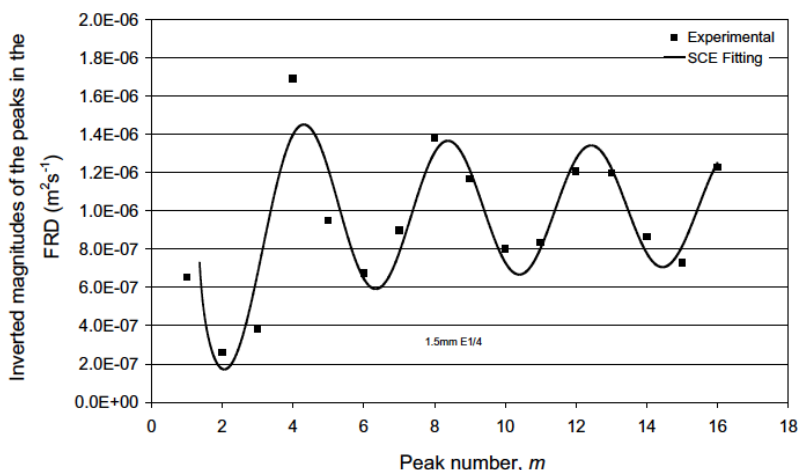

Figure 18: Dominant frequency extraction in inverted frequency response diagram peaks for antisymmetric system with leak located 9.39m from upstream boundary.

It is important to point out that the regression process provides a single frequency decomposition of the data set. This procedure should not be confused with conventional inverse transient analysis where a good match is indicative of a good leak location procedure. Instead, the procedure should be considered as an alternative to Fourier decomposition of the data, where small distortions in the data that do not constitute a sinusoidal pattern (hence not leak related) are ignored in the search for the dominant oscillation. This provides the technique with a degree of resistance to random data contamination.

The FRD from an intact pipeline with no leaks in an antisymmetric system is also shown in Fig. 19. This FRD does not display an oscillatory pattern as in the leaking examples. Applying the SCE algorithm to

this result gives an oscillation with a frequency that lies close to zero, indicating that there is no dominant oscillatory component in the data. In addition, the FRD predicted by the transfer matrix model incorporating Zielke (1968) or Vardy and Brown (1995) unsteady friction are also shown with the experimental results of Figs 15, 17 and 19. For all leaking cases the position of the resonant peaks in the FRD correctly matches the results predicted by the numerical model and validates this linear systems approach for the determination of the modal behaviour of a pipeline system. However, deviations are observed in the magnitude of the peaks and may be due to a number of factors, such as small imperfections within the pipe and inability of the existing transient models to replicate exactly the pipeline behaviour. It should be noted, however, that this discrepancy between the model and experimental result does not have an impact on the applicability of the proposed leak detection method. The FRD approach targets the specific influence of leaks on the transient behavior and does not require the accurate modelling of transients within the pipe in order to detect and locate leaks as shown in the above results.
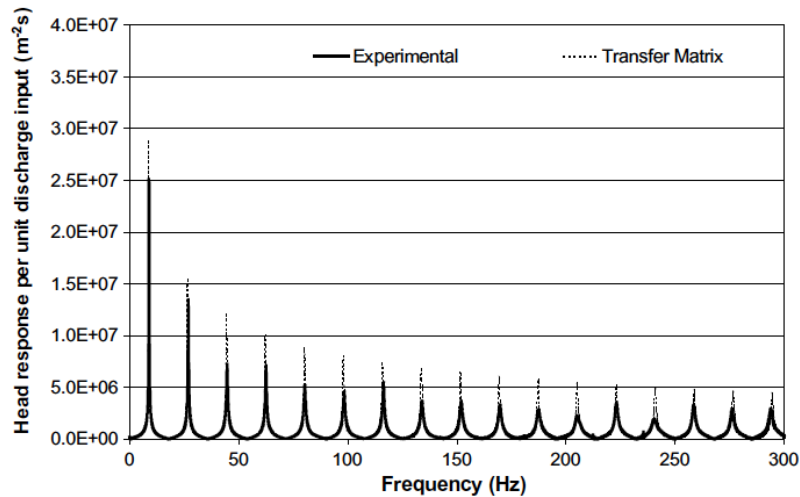

Figure 19: The frequency response diagram from an intact pipeline in an antisymmetric configuration.

5.3 Impact of significant background noise

The proposed FRD method of leak detection is more robust with respect to background noise than conventional time domain methods of leak detection due to the following intrinsic properties:

1. The cross-correlation between the input and output signal during the extraction of the FRD using Eq. (1) minimizes all signal contamination that is not of the same form as the input signal. This is commonly known as match filtering and is often applied in radar signal analysis (Lynn, 1982; Liou, 1998).
2. The fact that only the peaks of the FRD are used in the analysis means that only components of the signal that repeat at the fundamental frequency of the pipeline will have any bearing on the result. Random noise, which rarely occurs at the same position within each period of oscillation, will have a minimal impact on the accuracy of the final leak detection result.
3. Peaks in the FRD have a good signal to noise ratio since they contain more energy than other frequency components in the signal.

These effects are illustrated in the following example where the transient signal is strongly contaminated by background noise. The noise is generated artificially from a uniform distribution of a maximum magnitude of 1m. The noise is added to the original data from the symmetric test. The first two periods of the contaminated time series are shown in Fig. 20 with the original data. The contaminated trace displays a significant level of distortion and the leak-induced reflections are not well defined within the result. In comparison, the extracted FRD from this situation is shown in Fig. 21 and is compared with the uncontaminated FRD from Fig. 15. While the FRD of the contaminated signal contains a higher level of distortion than the FRD of the original signal, its effect is limited to responses at higher frequencies and also the non-harmonic portions of the FRD. The observable peaks in the contaminated FRD show responses that are identical to the uncontaminated data for the low frequencies peaks (up to 90 Hz), and the original leak-induced pattern is still clearly observable. The analysis of system behaviour in the frequency domain using the FRD provides higher tolerance to system noise than its time domain counterpart.
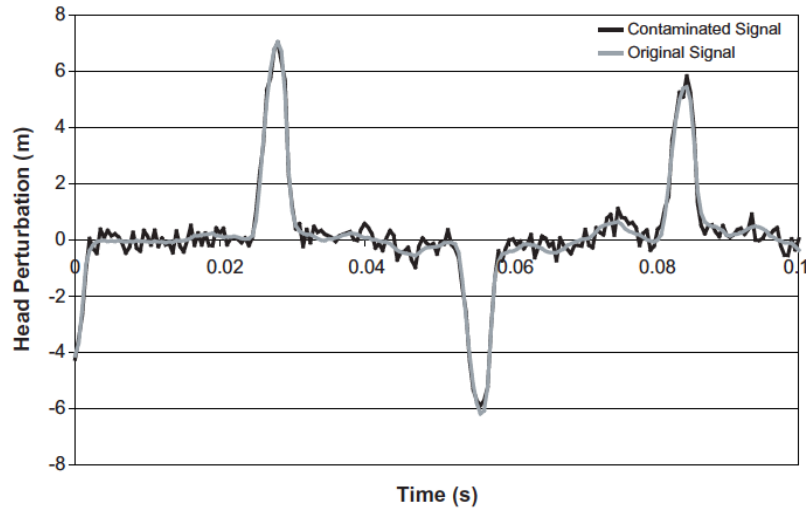
Figure 20: Time series of transient generated in high noise conditions, for a symmetric boundary with leak located 6.695 m from reservoir boundary.
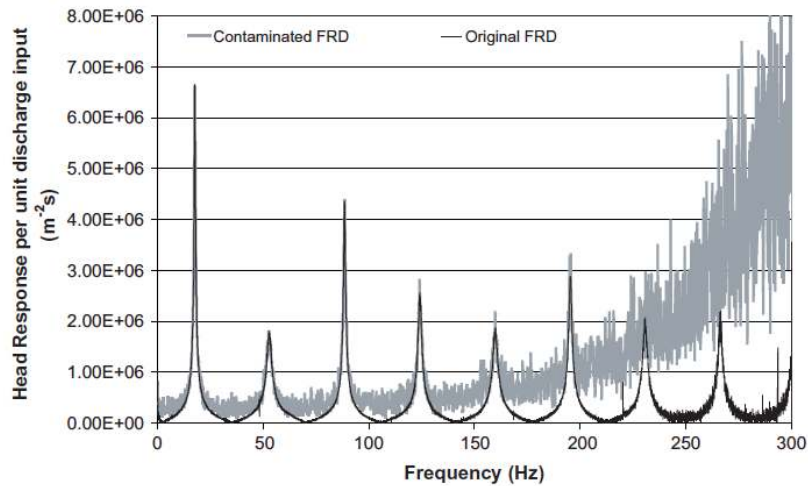

Figure 21: Frequency response diagram (FRD) generated in high noise conditions, for a symmetric boundary with leak located 6.695m from reservoir boundary.

6 Scope of application

This section presents the generalization of the technique in order to apply it to a wider range of system configurations. The limitations of the method are also discussed.

6.1 Network applications

The extraction of the FRD for a pipeline section and the subsequent leak detection methodology relies on the pipeline lying between by well-defined boundaries with the excitation valve at one end and a reservoir at the other. However, few systems exist within this narrow definition; many contain multiple pipe sections or exist as complex networks. Lee et al. (2005b) illustrated how the FRD method can be expanded for a network situation. It involves the decomposition of complex pipe systems into individual single pipes where the FRD of each pipe can be extracted to determine its integrity. Lee et al. (2005b) presented details of this procedure in a numerical investigation.

6.2 Multiple leaks

Lee et al. (2003) have illustrated numerical results where the proposed technique can be expanded for multiple leaks in a system excited by an inline valve. In the same way, the equations presented in this paper (using a side-discharge exciter) can be expanded for multiple-leak cases. For a symmetric boundary, Eq. (11) becomes

$$\frac{1}{|h_{n_2}|} = \sum_{i-1}^{n_{leak}} \frac{Q_{LO_i}}{4H_{LO_i}} (1 - \cos(4\pi m x_{Li}^* - 2\pi x_{Li}^*)) \tag{18}$$

where n_{leak} denotes the total number of leaks. For an antisymmetric boundary, Eq. (13) becomes,

$$\frac{1}{|h_{n_5}|} = \sum_{i-1}^{n_{leak}} \frac{Q_{LO_i}}{4H_{LO_i}} (1 - \cos(2\pi m x_{Li}^* - \pi x_{Li}^*)) + \frac{Q_{VO}}{2\Delta H_{VO}} \tag{19}$$

Each leak generates its own oscillation frequency on the peaks and the final result is a linear summation all these oscillations. Lee et al. (2003) have shown the accurate detection, location and sizing of up to three leaks within a single pipeline using the FRD. Note that as described in the original derivations, the equations are bounded by the approximation where the sum of $(Q_{L0}a)/(4H_{L0}gA)$ over all the leaks is $\ll 1$. While the violation of this criterion does not affect the application of the technique as such, however, a violation will impose additional small amplitude oscillations onto the peaks that may be mistaken for small leaks. These small additional frequencies, however, are of a smaller magnitude than the main frequency and their presence do not affect the accuracy in predicting the true leak. In addition, the properties of these additional oscillations can be determined once the leak position is known and the elimination of these oscillations as possible leaks is possible.

6.3 Limitations of the technique

A limitation of this technique is the dependence upon the bandwidth of the input signal in relation to the fundamental frequency for the pipeline. For the experimental apparatus in the University of Adelaide, the short pipe length meant that its fundamental frequency is high in relation to the bandwidth of the input signal, leading to a small number of peaks that can be used for the analysis. The low number of data points places a limit on the lowest frequency that can be detected within the system. For eight data points, the lowest frequency that can be detected is one that undergoes a quarter of its cycle within this number of data, corresponding to a frequency of 0.03125. Any frequency lower than this value would appear as a trend in the data.

Longer pipe lengths in field application give a much lower fundamental frequency than that in the experimental apparatus. For the same input signal bandwidth (which is possible in such systems), many more harmonic peaks are observable than in the experimental system. In addition, the scale of the laboratory apparatus also results in dominant unsteady friction effects and possible structural vibration problems that are relatively small in larger-scale systems.

The nature of the technique also means that leaks located near particular positions within the pipeline generate weak oscillations within the FRD peaks and, therefore, cannot be detected. For a symmetric system, these positions are the system boundaries, the quarter points and the midpoint of the system. In the antisymmetric case leaks at the boundary and at the midpoint cannot be detected. This technique assumes an optimum configuration of the measurement transducer and the transient source. A numerical investigation into the effect of deviating from this configuration is presented in Lee et al. (2005a) along with a correction procedure for non-optimum configurations. Note that the smallest leak that can be detected in a pipeline system is dependent on the magnitude and the structure of background noise and should only be determined in situ on a case-by-case basis.

7 Conclusion

Under small transient perturbations a pipeline system can be considered and modelled as a linear system and the system behavior can be summarized by an FRD. Leaks create an oscillation in the peaks of the FRD and the properties of this oscillation provide information as to the location of leaks. Experimental tests, conducted at the University of Adelaide under different boundary condition configurations verified the method. The technique has three distinct advantages over other leak detection methods:

1. It has the ability to determine the presence of a leak without comparing to a preexisting "no-leak"

benchmark for the system.
2. The leak detection procedure does not require forward modelling of the system and knowledge of system parameters such as pipe roughness, pipe size and the extent of the unsteady frictional effect need not be known.
3. It is robust with respect to system noise.

The optimum position of the transient source and the measurement transducers for symmetric boundary conditions is at the centre of the system; for antisymmetric boundary conditions it is next to the high impedance boundary. A shift in the selection of the input parameter from the previously used dimensionless valve opening to the induced discharge perturbation has removed previous limitations based on the size of the valve movement. Good matches between the MOC and the linear transfer matrix equations indicate that non-linear behaviour is not a limitation.

Notation
a = Wave speed
A = Area of pipeline
A_L = Area of leak orifice
C_d = Coefficient of discharge for leak orifice
C_v = Loss coefficient for valve opening
D = Diameter of pipeline
f = Darcy–Weisbach friction factor or frequency in the peaks of the FRD
g = Gravitational acceleration
h = Complex hydraulic grade line perturbation
$|h|$ = Magnitude of head perturbation
H = Hydraulic grade line elevation or frequency response function
ΔH = Change in the head at the transient generating point
ΔH_{V0} = Steady-state head loss across the valve
H_{L0} = Steady-state head at the leak
i = Imaginary unit, $\sqrt{-1}$
l = Length of pipe section
L = Total length of pipeline
m = Frequency of the peak oscillation, in terms of "per peak interval"
q = Complex discharge perturbation
Q = Discharge
ΔQ = Change in the discharge at the transient generating point
Q_{L0} = Steady-state flow out of the leak
Q_{V0} = Steady-state flow through the valve
R = Correlation function
S = Fourier transform of the correlation function, R or the scale correction function
T = Trend correction function
t = Time
U = Overall transfer matrix for the pipeline system excluding the oscillating valve
x = Distance along pipe or the input to the system
X = Fitted parameters
x_L = Position of leak measured from upstream boundary
x_L^*= Dimensionless position of leak, given by xL/L
y = Output of the system (measured head response)
φ = Phase
τ = Dimensionless valve aperture size
ω = Frequency

References

1. Ambardar, A. (1999). Analog and Digital Signal Processing, 2nd edn., Pacific Grove, CA, USA.
2. Brunone, B. (1999). "Transient Test-Based Technique for Leak Detection in Outfall Pipes". J.Water Resour. Planning Manage. ASCE 125(5), 302–306.
3. Chaudhry, M.H. (1970). "Resonance in Pressurized Piping Systems". J. Hydraul. Div. ASCE 96(HY9), 1819–1839.
4. Chaudhry, M.H. (1987). Applied Hydraulic Transients. Van Nostrand Reinhold Company Inc.,

NewYork.

5. Covas, D. and Ramos, H. (1999). "Leakage Detection in Single Pipelines Using Pressure Wave Behaviour". Water Ind. System Modelling Optimisation Appl. 1, 287–299.

6. Covas, D., Graham, N., Maksimovic, C., Kapelan, Z., Savic, D. and Walters, G. (2003). "An Assessment of the Application of Inverse Transient Analysis for Leak Detection: Part II— Collection and Application of Experimental Data". In: Maksimovic, C. and Graham, N. (eds), Proceedings of Computer Control for Water Industry (CCWI), London, UK.

7. Ferrante, M., Brunone, B. and Rossetti, A.G. (2001). "Harmonic Analysis of Pressure Signal During Transients for Leak Detection in Pressurized Pipes". BHR Group. In: 4th International Conference on Water Pipeline System— Managing Pipeline Assets in an Evolving Market, York, UK, 28–30 March.

8. Jönsson, L. and Larson, M. (1992). "Leak Detection Through Hydraulic Transient Analysis". In: Coulbeck, B. Frequency response method for pipeline leak detection 707 and Evans, E. (eds), Pipeline Systems, Kluwer Academic Publishers, Dordrecht, pp. 273–286.

9. Kapelan, S.Z., Savic, D.A., Walters, G.A., Covas, D., Stoianov, I., Graham, N., Maksimovic, C. and Butler,D. (2003). "Inverse Transient Analysis in Pipe Networks for Leakage Detection, Quantification and Roughness Calibration". In: Proceedings of the 30th IAHR Congress, Thessaloniki, Greece.

10. Lee, P.J., Vitkovský, J.P., Lambert, M.F., Simpson, A.R. and Liggett, J.A. (2002a). "Leak Detection in Pipelines Using an Inverse Resonance Method". In: 2002 Conference on Water Resources Planning and Management, ASCE, Virginia, USA, 19–22 May [CDROM].

11. Lee, P.J., Vitkovský, J.P., Lambert, M.F., Simpson, A.R. and Liggett, J.A. (2002b). Discussion of "Leak Detection in Pipes by Frequency Response Method Using a Step Excitation by Witness Mpesha, M. Hanif Chaudhry, and Sarah L. Gassman". J. Hydraul. Res. 40(1), 55–62.

12. Lee, P.J., Vitkovský, J.P., Lambert, M.F., Simpson, A.R. and Liggett, J.A. (2003). "Frequency Response Coding for the Location of Leaks in Single Pipeline Systems". International Conference on Pumps, Electromechanical Devices and Systems Applied to Urban Water Management, IAHR and IHR, Valencia, Spain, April 22–25.

13. Lee, P.J., Vitkovský, J.P., Lambert, M.F., Simpson, A.R. and Liggett, J.A. (2005a). "Leak Location Using the Pattern of the Frequency Response Diagram in Pipelines: a Numerical Study". J. Sound Vibration 284(3), 1051–1073.

14. Lee, P.J., Vitkovský, J.P., Lambert, M.F., Simpson, A.R. and Liggett, J.A. (2005b). "Detecting Pipeline Leaks Using the Frequency Response Diagram". J. Hydraul. Engng. ASCE 131(7), 596–604.

15. Liggett, J.A. and Chen, L.C. (1994). "Inverse Transient Analysis in Pipe Network". J. Hydraul. Engng. ASCE 120(8), 934–955.

16. Liou, C.P. (1998). "Pipeline Leak Detection by Impulse Response Extraction". J. Fluids Engng. ASME 120, 833–838.

17. Lynn, P. (1982). An Introduction to the Analysis and Processing of Signals. The Macmillan Press Ltd, London and Basingstoke.

18. Mpesha, W., Chaudhry, M. and Gassman, S. (2002). "Leak Detection in Pipes by Frequency Response Method Using a Step Excitation". J. Hydraul. Res. IAHR 40(1), 55–62.

19. Mpesha,W., Gassman, S.L. and Chaudhry, M.H. (2001). "Leak Detection in Pipes by Frequency Response Method". J. Hydraul. Engng. ASCE 127(2), 134–147.

20. Nash, G. and Karney, B. (1999). "Efficient Inverse Transient Analysis in Series Pipe Systems". J. Hydraul. Engng. ASCE 125(7), 761–764.

21. Suo, L. andWylie, E. (1989). "Impulse Response Method for Frequency Dependent Pipeline Transients". J. Fluids Engng. ASME 111(12), 478–483.

22. Vardy, A.E. and Brown, J.M.B. (1995). "Transient, Turbulent, Smooth Pipe Friction". J. Hydraul. Res. IAHR 33(4), 435–456.

23. Vitkovský, J.P., Simpson, A.R. and Lambert, M.F. (1999). "Leak Detection and Calibration of Water Distribution System Using Transient and Genetic Algorithms". Water Distribution System Conference, Division of Water Resource Planning and Management, ASCE, Tempe, Arizona, 7–9 June.

24. Vitkovský, J.P., Bergant, A., Simpson, A.R. and Lambert, M.F. (2003). "Steady Oscillatory Flow Solution Including Unsteady Friction". In: International Conference on Pumps, Electromechanical Devices and Systems Applied to Urban Water Management, IAHR and IHR, Valencia, Spain, April 22–25.

25. Wang, X.J., Lambert, M.F., Simpson, A.R., Liggett, J.A. and V.tkovský, J.P. (2002). "Leak

Detection in Pipeline Systems Using the Damping of Fluid Transients". J. Hydraul. Engng. ASCE 128(7), 697–711.

26. Zielke, W. (1968). "Frequency-Dependent Friction in Transient Pipe Flow". J. Basic Engng. ASME 90, 109–115.